doi:10.1093/brain/awy277 BRAIN 2018: 141; 3457–3471 | 3457

BRAIN
A JOURNAL OF NEUROLOGY

Neurobiological substrates underlying the effect of genomic risk for depression on the conversion of amnestic mild cognitive impairment

Jiayuan Xu,[1,*] Qiaojun Li,[2,*] Wen Qin,[1,*] Mulin Jun Li,[3] Chuanjun Zhuo,[1,4] Huaigui Liu,[1] Feng Liu,[1] Junping Wang,[1] Gunter Schumann[5,6] and Chunshui Yu[1,7] on behalf of the Alzheimer's Disease Neuroimaging Initiative

*These authors contributed equally to this work.

Depression increases the conversion risk from amnestic mild cognitive impairment to Alzheimer's disease with unknown mechanisms. We hypothesize that the cumulative genomic risk for major depressive disorder may be a candidate cause for the increased conversion risk. Here, we aimed to investigate the predictive effect of the polygenic risk scores of major depressive disorder-specific genetic variants (PRS_{sMDD}) on the conversion from non-depressed amnestic mild cognitive impairment to Alzheimer's disease, and its underlying neurobiological mechanisms. The PRS_{sMDD} could predict the conversion from amnestic mild cognitive impairment to Alzheimer's disease, and amnestic mild cognitive impairment patients with high risk scores showed 16.25% higher conversion rate than those with low risk. The PRS_{sMDD} was correlated with the left hippocampal volume, which was found to mediate the predictive effect of the PRS_{sMDD} on the conversion of amnestic mild cognitive impairment. The major depressive disorder-specific genetic variants were mapped into genes using different strategies, and then enrichment analyses and protein–protein interaction network analysis revealed that these genes were involved in developmental process and amyloid-beta binding. They showed temporal-specific expression in the hippocampus in middle and late foetal developmental periods. Cell type-specific expression analysis of these genes demonstrated significant over-representation in the pyramidal neurons and interneurons in the hippocampus. These cross-scale neurobiological analyses and functional annotations indicate that major depressive disorder-specific genetic variants may increase the conversion from amnestic mild cognitive impairment to Alzheimer's disease by modulating the early hippocampal development and amyloid-beta binding. The PRS_{sMDD} could be used as a complementary measure to select patients with amnestic mild cognitive impairment with high conversion risk to Alzheimer's disease.

1 Department of Radiology and Tianjin Key Laboratory of Functional Imaging, Tianjin Medical University General Hospital, Tianjin 300052, P.R. China
2 College of Information Engineering, Tianjin University of Commerce, Tianjin 300052, P.R. China
3 Collaborative Innovation Center of Tianjin for Medical Epigenetics, Tianjin Key Laboratory of Medical Epigenetics, Department of Pharmacology, Tianjin Medical University, Tianjin 300052, P.R. China
4 Department of Psychiatry Functional Neuroimaging Laboratory, Tianjin Mental Health Center, Tianjin Anding Hospital, Tianjin 300052, P.R. China
5 Institute of Psychiatry, Psychology and Neuroscience, King's College London, London SE5 8AF, UK
6 Medical Research Council Social, Genetic and Developmental Psychiatry Centre, London SE5 8AF, UK

Received April 12, 2018. Revised August 27, 2018. Accepted September 12, 2018. Advance Access publication November 14, 2018

7 CAS Center for Excellence in Brain Science and Intelligence Technology, Chinese Academy of Sciences, Shanghai, 200031, P.R. China

Correspondence to: Chunshui Yu, PhD
Department of Radiology, Tianjin Medical University General Hospital, No. 154, Anshan Road, Heping District, Tianjin 300052, China
E-mail: chunshuiyu@tijmu.edu.cn

Keywords: amnesic mild cognitive impairment conversion to Alzheimer's disease; hippocampal volume; major depressive disorder; neurobiological mechanisms; polygenic risk scores

Abbreviations: aMCI(-C/S) = amnestic mild cognitive impairment (-conversion to Alzheimer's disease/stable diagnosis); GO = gene ontology; MDD = major depressive disorder; PPI = protein–protein interaction; $PRS_{AD/MDD/sAD/sMDD/stAD}$ = polygenic risk scores for Alzheimer's disease/major depressive disorder/Alzheimer's disease-specific/major depressive disorder-specific/top 1806 Alzheimer's disease-specific genetic variants; SNP = single-nucleotide polymorphism

Introduction

The amnestic mild cognitive impairment (aMCI) is a state of cognitive deficit that is not severe enough to fulfil the criteria of dementia (Winblad *et al.*, 2004) and shows a much higher probability of developing into Alzheimer's disease (Palmer *et al.*, 2008). Identifying biological measures with the potential to predict the conversion from aMCI to Alzheimer's disease is clinically important for early interventions of Alzheimer's disease. In the past decades, a variety of demographic (Tokuchi *et al.*, 2014), clinical (Mazzeo *et al.*, 2016), cognitive (Julayanont *et al.*, 2014), neuroimaging (Yuan *et al.*, 2009), and genetic measures (Rodriguez-Rodriguez *et al.*, 2013; Adams *et al.*, 2015) have been proposed as candidate measures for the prediction. Among these measures, a lifetime history of major depressive disorder (MDD) (Jorm, 2001), the presence of depressive symptom (Kida *et al.*, 2016; Mourao *et al.*, 2016; Sacuiu *et al.*, 2016; Barca *et al.*, 2017), or the coexistence of a diagnosis of MDD (Modrego and Ferrandez, 2004) has been found to increase the conversion risk from aMCI to Alzheimer's disease, despite of non-significant findings (Palmer *et al.*, 2010; De Roeck *et al.*, 2016). However, few studies have investigated why depression could increase the conversion risk from aMCI to Alzheimer's disease.

Besides social-psychological factors, such as stressful life events (Park *et al.*, 2015) and interpersonal dysfunction (Hames *et al.*, 2013), genome-wide association studies (GWAS) reveal a role of genetic factors in MDD (Ripke *et al.*, 2013). In terms of genetics, one possibility for the association between MDD and the conversion of aMCI is that MDD and Alzheimer's disease may share common genetic variants. This idea is supported by candidate gene studies (Skoog *et al.*, 2015; Ye *et al.*, 2016), but is not supported by the polygenic score analyses (Bulik-Sullivan *et al.*, 2015*a*; Power *et al.*, 2017). An alternative possibility is that the MDD- and Alzheimer's disease-specific genetic variants may affect the same biological pathways, processes, cells, or structures via different mechanisms at different developmental periods. Thus, this study aimed to investigate if the cumulative MDD-specific genetic risk could predict the conversion from aMCI to Alzheimer's disease. If so, we explored the possible neurobiological mechanisms underlying the predictive effect further.

The cumulative genetic risk for MDD could be assessed by the polygenic risk scores (PRS) for this disorder (PRS_{MDD}) (Milaneschi *et al.*, 2016) and the cumulative genetic risk for Alzheimer's disease could be evaluated by the PRS_{AD} (Sabuncu *et al.*, 2012). Although many studies have used the PRS_{MDD} to predict MDD (Holmes *et al.*, 2012; Milaneschi *et al.*, 2016; Gibson *et al.*, 2017; Qiu *et al.*, 2017) and applied the PRS_{AD} to predict Alzheimer's disease (Escott-Price *et al.*, 2015; Mormino *et al.*, 2016) and the conversion from aMCI to Alzheimer's disease (Rodriguez-Rodriguez *et al.*, 2013; Adams *et al.*, 2015), no studies have used the PRS_{MDD} to predict the conversion from aMCI to Alzheimer's disease. To exclude the possibility that the predictive effect of the PRS_{MDD} on the conversion is driven by genetic variants common to MDD and Alzheimer's disease, we only used genetic variants specific to MDD to calculate PRS_{sMDD} by excluding common genetic variants of the two disorders. If a significant predictive effect existed, we investigated neuroanatomical substrates underlying such a prediction. The identified genetic variants were fine-mapped into genes using different strategies, and then enrichment and protein–protein interaction network analyses were performed to identify potential functions of these genes. Temporal- and cell type-specific expression analyses were finally used to explore in which developmental periods and cell types these genes are significantly expressed. A schematic summary of the study design is shown in Fig. 1.

Materials and methods

Discovery and target samples

The PRS calculation requires a discovery sample and a target sample. The discovery sample was used to identify effect size of a set of genetic variants that were nominally associated with the disease status at a predefined *P*-value. Then, the PRS was calculated for each subject in the target sample to estimate

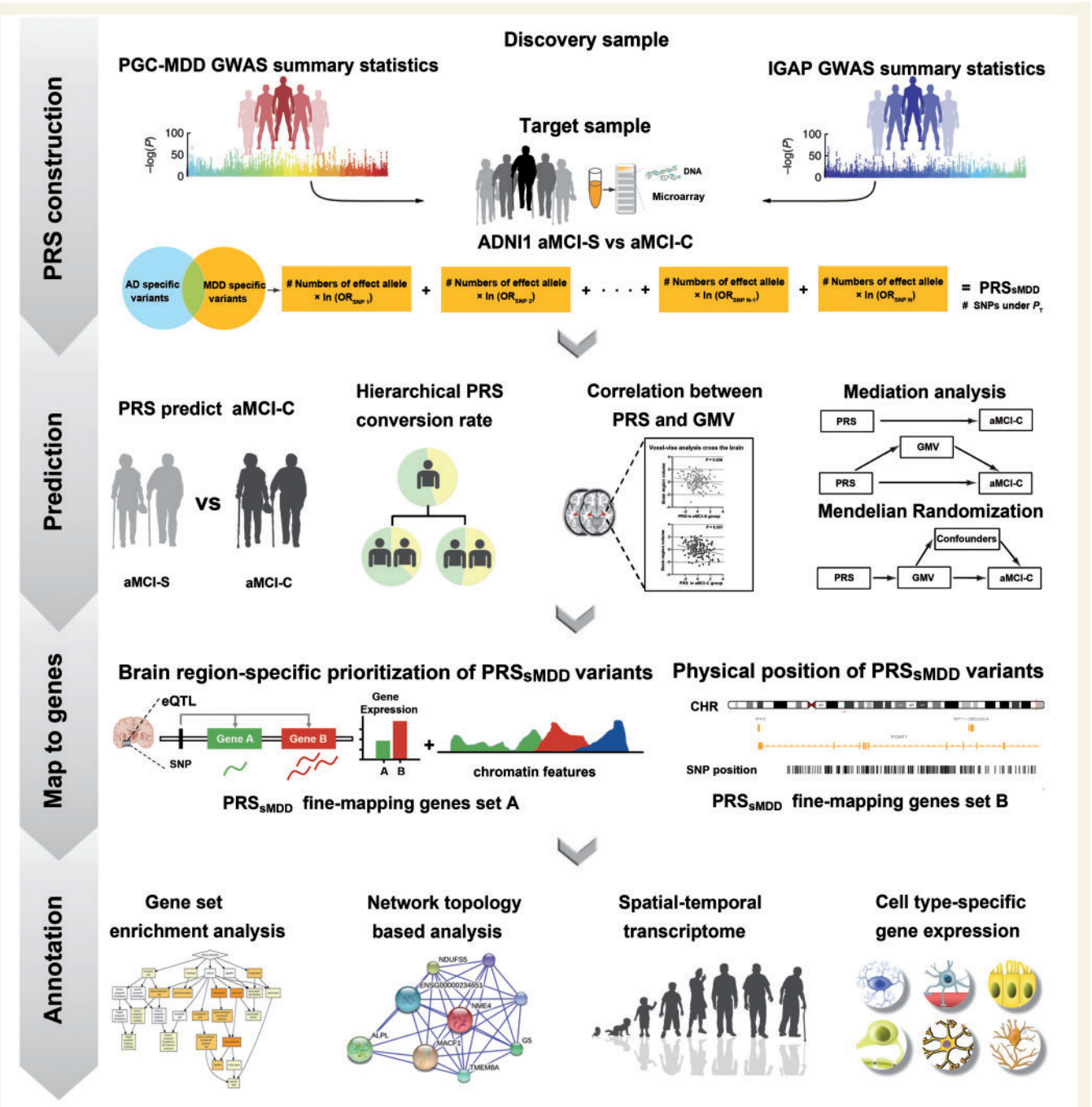

Figure 1 A schematic summary of the study design. ADNI = Alzheimer's Disease Neuroimaging Initiative; CHR = chromosome; eQTL = expression quantitative trait loci; GMV = grey matter volume; GWAS = genome-wide association studies; IGAP = International Genomics of Alzheimer's Project; OR = odd ratios; PGC-MDD = major depressive disorder working group of Psychiatric Genomics Consortium; P_T = *P*-values threshold of genome-wide association studies.

cumulative genetic risk of this subject for the disease. GWAS data of the Psychiatric Genomics Consortium (PGC) (Sullivan, 2010) and International Genomics of Alzheimer's Project (IGAP) (Lambert *et al.*, 2013) were used as the discovery samples to calculate PRS_{MDD} and PRS_{AD}, respectively. The target sample included 398 non-depressed (with a geriatric depression scale < 6) aMCI patients provided by the first stage of Alzheimer's disease Neuroimaging Initiative (ADNI-1). The detailed information about the discovery and target samples is provided in the Supplementary material.

Genotyping

For the 757 subjects from ADNI-1, the genome-wide single-nucleotide polymorphisms (SNPs) were genotyped using the Illumina Human610-Quad Bead chip.

Quality control

In individual-level quality control, we excluded subjects with a missing genotyping rate >0.05, sex inconsistency, possible relative relationships, and being European population outliers identified by multidimensional scaling (MDS). In SNP-level quality control, we excluded SNPs with a missing call rate >0.05, minor allele frequency <0.01, significant deviation from Hardy-Weinberg equilibrium, and ambiguous strand. Finally, imputation was performed using MaCH (Li *et al.*, 2010) and MiniMac (Howie *et al.*, 2012). Detailed information of quality control and imputation is shown in the Supplementary material.

Polygenic risk score calculation

The PRS is used to assess the cumulative genetic risk for a certain disorder (Purcell *et al.*, 2009). In the discovery sample, we calculated the association between SNPs and disease status at a predefined *P* threshold (P_T). Under a certain P_T, we then removed the effects of SNPs in linkage disequilibrium (LD) in each clumped region (excluding SNPs with $r^2 > 0.25$ within a 250-kb window) and selected the index SNPs with the most significant *P*-value from each clumped association region based on the discovery sample. Thus, we obtained the information of the risk alleles and effect sizes of the index SNPs for each P_T value. In the target sample, the PRS was calculated for each individual as the sum of the count of risk alleles multiplied by the corresponding effect sizes (natural log of the odds ratio) across these index SNPs.

To identify the P_T value that could generate PRS with the best prediction for the conversion from aMCI to Alzheimer's disease, the PRSice software (http://prsice.info) (Euesden *et al.*, 2015) was used to generate 1000 PRS values for P_T ranging from 0.001 to 1 with an increment of 0.001, while controlling for sex, age and educational years at baseline, the number of *APOE* ε4, and the first four MDS components for population stratification. $P_T = 1$ indicates that all SNPs of the discovery sample are included to calculate the PRS in the target sample. By evaluating the predictive abilities, we could obtain the best P_T values for calculating PRS_{MDD} and PRS_{AD} in the target sample. Using the best P_T values, we could obtain the risk alleles and effect sizes of the index SNPs for calculating the PRS_{MDD} and PRS_{AD} in the target sample. The PRS_{MDD} and PRS_{AD} were computed for each aMCI patient and then *z*-transformed for visualization.

To exclude the possibility that the predictive effect of PRS_{MDD} on the aMCI conversion is driven by genetic variants common to MDD and Alzheimer's disease, we calculated PRS specific to MDD (PRS_{sMDD}) only using genetic variants specific to MDD by excluding common variants of the two disorders. In the same way, we also calculated PRS specific to Alzheimer's disease (PRS_{sAD}). LD score regression (Bulik-Sullivan *et al.*, 2015*b*) and co-localization analyses (Giambartolomei *et al.*, 2014; Pickrell *et al.*, 2016) were additionally performed to validate the specificity of index SNPs to MDD rather than Alzheimer's disease (Supplementary material).

Image acquisition

Subjects were scanned with a standardized MRI protocol developed for ADNI (Jack *et al.*, 2008). Details about the rationale and development of the standardized MRI datasets have been previously described (Wyman *et al.*, 2013). The high resolution structural MRI data were acquired at 59 sites using 1.5 T MRI scanners with a sagittal 3D magnetization prepared rapid acquisition gradient echo sequence (http://adni.loni.ucla.edu).

Grey matter volume calculation

All structural images were visually checked by two radiologists. The preprocessing processes of structural images included segmentation, normalization, modulation, and smoothing (Supplementary material). The specific reasons for exclusion for patients with aMCI are shown in Supplementary Table 1. Finally, 322 aMCI patients with qualified genotyping and neuroimaging data were included and divided into conversion (aMCI-C, $n = 187$) and stable (aMCI-S, $n = 135$) groups. The demographic and genetic data of these patients are shown in Table 1.

Statistical analyses

Demographic data

The demographic data were analysed using the Statistical Package for the Social Sciences version 18.0 (SPSS Inc., Chicago, Illinois, USA). The chi-square or *t*-test was used to compare differences in sex, age, educational years, geriatric

Table 1 Demographic and genetic characteristics of the target sample

Demographic variables	aMCI-S (*n* = 135)	aMCI-C (*n* = 187)	Statistics	*P*
Age at baseline, y	75.64 (7.16)	74.50 (7.21)	1.99	0.16
APOE ε4 carriers[a], *n*	62	120	10.62	$\mathbf{1.10 \times 10^{-3}}$
Educational years	15.50 (3.12)	15.73 (2.89)	0.46	0.50
Males, *n*	90	120	0.22	0.37
GDS	1.63 (1.38)	1.59 (1.36)	0.07	0.79
PRS_{AD}[b]	−0.41 (0.88)	0.30 (0.98)	44.04	$\mathbf{1.37 \times 10^{-10}}$
PRS_{MDD}[b]	−0.20 (0.97)	0.28 (0.97)	19.35	$\mathbf{1.48 \times 10^{-5}}$
PRS_{sAD}[b]	−0.40 (0.88)	0.29 (0.98)	42.59	$\mathbf{2.65 \times 10^{-10}}$
PRS_{sMDD}[b]	−0.16 (0.97)	0.22 (1.00)	11.96	$\mathbf{6.18 \times 10^{-4}}$
$PRS_{sMDD+AD}$[b]	−0.40 (0.89)	0.31 (0.98)	43.63	$\mathbf{1.29 \times 10^{-10}}$

Data are shown as mean (SD). AD = Alzheimer's disease; GDS = Geriatric Depression Scale.

[a]*APOE* ε4 carriers include subjects with one or two copies of ε4 allele at the *APOE* locus.

[b]The PRS are *z*-transformed for visualization.

P-values in bold indicate there are significant differences between groups.

depression scale, and PRS measures between the aMCI-S and aMCI-C groups.

Polygenic risk analysis

The logistic regression was used to predict odds of the aMCI-C using the PRS calculated under each of the 1000 P_T thresholds. The permutation test ($P < 0.05$) was used to correct multiple comparisons. Nagelkerke's pseudo R^2 was calculated to measure the proportion of variance explained by the PRS. A Cox proportional hazard model was used to explore the relations between the PRS and the conversion at the different time points, with the age and educational years at baseline, the sex, the number of *APOE* ε4, and the PRS as independent variables. For the best-fitting PRS, hazard ratios (HRs) for these variables were calculated using the prediction models.

The 322 aMCI patients were bisected according to their PRS_{sMDD} or PRS_{sAD}; we defined 161 patients with relatively low PRS as low PRS group and another 161 patients as high PRS group. The chi-square test was used to compare differences in conversion rate of aMCI among the four hierarchical risk groups (double low risk, low PRS_{sAD} but high PRS_{sMDD}, high PRS_{sAD} but low PRS_{sMDD}, and double high risk groups). The 322 aMCI patients were also trisected according to their PRS_{sMDD} or PRS_{sAD}, the bottom third (107 patients) was defined as the low-risk group, the middle third (107 patients) as the middle-risk group, and the upper third (108 patients) as the high-risk group. We also compared differences in conversion rate among the nine hierarchical risk groups.

Imaging data

The voxel-wise multiple regression analysis was performed to identify brain regions whose grey matter volumes were significantly correlated with PRS_{sMDD} using Statistical Parametric Mapping software package (SPM8, http://www.fil.ion.ucl.ac.uk/spm), while controlling for the effect of neuroimaging sites. Multiple comparisons were corrected using a voxel-level family-wise error (FWE) method ($P_c < 0.05$, cluster size >200 voxels). The grey matter volumes of brain regions with significant correlations with the PRS_{sMDD} were extracted for further analysis.

Mediation analysis and Mendelian randomization

The mediation analysis was performed to test whether the grey matter volume of each significant region mediates the association between PRS_{sMDD} and the conversion of aMCI (Preacher and Hayes, 2008; Hayes, 2013). The PRS_{sMDD} was defined as an independent variable, the grey matter volume of each significant region as a mediator variable, and the aMCI group assignment (aMCI-S versus aMCI-C) as a binary dependent variable. In addition, both a conventional two-stage Mendelian randomization method and a Mendelian randomization-Egger sensitivity analysis (http://www.mendelianrandomization.com/index.php/software-code) were applied using PRS_{sMDD} as instrumental variable to make causal inference between the grey matter volume of each significant region and aMCI conversion (Burgess and Thompson, 2013, 2015; Burgess, 2014) (Supplementary material).

Fine-mapping MDD-specific genetic variants into genes

The context-dependent epigenomic weighting for prioritization of variants (CEPIP) (Li *et al.*, 2017) was used to estimate the brain region-specific regulatory probability of each PRS_{sMDD} genetic variant by integrating the expression quantitative trait loci (eQTLs) (Brown *et al.*, 2013) and epigenomic features in the specific human brain tissues (Kundaje *et al.*, 2015). The PRS_{sMDD} genetic variants were weighted by the brain region-specific regulatory probability, and were then fine-mapped into genes using gene-based association test (GATES) (within a 5-kb window) in the human reference assembly (GRch37/hg19) (Li *et al.*, 2011). As a result, we could identify genes that increase MDD susceptibility through brain region-specific functionally regulatory mechanisms. To exclude the bias derived from introducing brain region-specific biological information, we also fine-mapped PRS_{sMDD} genetic variants into genes only based on physical position of each variant (within a 5-kb window) and re-performed the analyses.

Gene enrichment analyses

The functions of these genes were annotated by identifying significant enrichments using the WebGestalt (http://www.webgestalt.org/option.php) (Wang *et al.*, 2017) and Gorilla (http://cbl-gorilla.cs.technion.ac.il) (Eden *et al.*, 2007, 2009). The Benjamini and Hochberg method for false discovery rate (FDR-BH correction) ($q_c < 0.05$) was applied to correct for multiple comparisons. The reference gene list included 18 774 genes derived from fine-mapping of all imputed SNPs of PGC-MDD and ADNI datasets.

Network topology-based analysis

The WebGestalt software was also used to perform the network topology-based analysis based on the human protein–protein interaction (PPI) of the Biological General Repository for Interaction Datasets (BIOGRID). All fine-mapping genes were firstly mapped to the PPI network of the BIOGRID; and the tightly connected genes (a portion of the candidate genes) formed a new PPI network based on the assumption that the mechanistically important genes are likely to form tightly connected clusters whereas other genes tend to be randomly distributed in the network. The network topology-based analysis could create a score for each gene in the PPI network of the BIOGRID based on its overall proximity to the seed genes, where the proximity was measured by the random walk analysis (Kohler *et al.*, 2008). In the PPI network of the BIOGRID, the top 10 genes with the most functional similarity with seed genes were identified as neighbouring genes and included in the new PPI network. The constituent genes of the resulted network, including the tightly connected candidate genes and the top 10 neighbouring genes, were enriched in gene ontology (GO) items using the hypergeometric test ($q_c < 0.05$).

Temporal expression analysis

The precise regulation of the spatial and temporal gene expression plays a key role in brain development, maturation and

ageing. The CSEA was used to explore in which developmental periods these PRS_{sMDD}-related genes are specifically expressed (Xu *et al.*, 2014) (http://genetics.wustl.edu/jdlab/csea-tool-2/). The analysis was performed using the Fisher's exact test ($q_c < 0.05$) across developmental stages at a specificity index threshold (pSI) threshold of 0.05. If any genes showed specific expression in any developmental stage under the most stringent threshold of pSI = 0.001, the expression pattern of these genes would be depicted using Human Brain Transcriptome (Kang *et al.*, 2011). In our analysis, we only focused on temporal feature of these genes expressed in the significant brain regions of mediation analysis and Mendelian randomization.

Cell type-specific expression analysis

With the single-cell RNA-sequencing technique, a prior study has provided the detailed cell type-specific expression data of nine major cell types in the mouse brain regions (Zeisel *et al.*, 2015). The Fisher's exact test was used to identify in which cell types these PRS_{sMDD} fine-mapping genes were specifically expressed in a certain brain region. These tests resulted in the pSI for each cell type, and the *P* threshold represents how likely the gene set is specifically expressed in a given cell type relative to the other cell types.

Data availability

The data that support the findings of this study are available from the corresponding author upon reasonable request.

Results

PRS_{MDD} could predict the conversion from aMCI to Alzheimer's disease

When the PRS_{MDD} were calculated using seven broad P_T values for associations between SNPs and MDD, we found the PRS_{MDD} ($P_T = 0.05$) could predict the status of the aMCI-C ($P = 0.002$) (Fig. 2A) and explained 4.08% of variance for the aMCI-C based on 10 618 index SNPs. When the PRS_{MDD} were computed using a high resolution method, the PRS_{MDD} calculated at $P_T = 0.009$ showed the highest prediction ($P = 7.49 \times 10^{-5}$), explained 6.86% of variance based on 2559 index SNPs (Fig. 2B and Table 2). Compared with aMCI-S patients, aMCI-C patients had a significantly higher adjusted PRS_{MDD} ($P = 1.48 \times 10^{-5}$) (Fig. 2C and Table 1). Compared to the low risk group, the middle [HRs = 2.45, 95% confidence interval (CI) = 1.48–4.03, $P = 4.56 \times 10^{-4}$] and high (HRs = 2.68, 95% CI = 1.24–5.82, $P = 3.23 \times 10^{-4}$) risk groups had more than two times of risk for the aMCI-C. The Cox survival analysis showed that the middle and high risk groups had a higher proportion of the aMCI-C than the low risk group (Fig. 2D). Moreover, the middle and high risk groups (mean time to conversion 35.91 months) progressed more rapidly into Alzheimer's disease than the low risk group (mean time to conversion 42.75 months).

We also investigated the predictive effect of the PRS_{AD} on the aMCI-C to validate the PRS method and to provide a reference for the predictive effect of the PRS_{MDD}. The broad analysis showed that the PRS_{AD} calculated at $P_T = 0.4$ could predict the aMCI-C ($P = 1.20 \times 10^{-9}$) (Fig. 2E), explained 18.02% of variance in the aMCI-C based on 54 106 index SNPs. The high resolution analysis revealed that the PRS_{AD} computed at $P_T = 0.352$ showed the highest prediction ($P = 7.10 \times 10^{-10}$), explained 18.55% of variance based on 49 831 index SNPs (Fig. 2F and Table 2). The aMCI-C group showed higher PRS_{AD} than the aMCI-S group ($P = 1.37 \times 10^{-10}$) (Fig. 2G and Table 1). Compared to the low risk group, the middle (HRs = 1.55, 95% CI = 1.04–2.31, $P = 0.032$) and high (HRs = 3.35, 95% CI = 2.30–4.88, $P = 3.25 \times 10^{-10}$) risk groups had increased risk for the aMCI-C. Cox survival analysis showed that the high risk group had a much higher proportion of the aMCI-C than the low risk group (Fig. 2H). Sensitivity, specificity, accuracy, area under curve were also provided (Table 2) and the accuracy of the models was confirmed by 10-fold cross validation (Supplementary material and Supplementary Table 2). We also found that aMCI patients carrying *APOE* $\varepsilon 4$ showed an increased risk for the conversion than *APOE* $\varepsilon 4$ non-carriers (HRs = 1.78, 95% CI = 1.31–2.42, $P = 2.21 \times 10^{-4}$); however, the age, educational years at baseline, and sex were not associated with the conversion.

PRS_{sMDD} could independently predict the conversion from aMCI to Alzheimer's disease

After excluding overlapping SNPs ($n = 4711$) between PRS_{MDD} and PRS_{AD}, the PRS_{sMDD} could significantly predict the aMCI-C ($P = 0.002$) and explained 4.19% of variance for the aMCI-C based on 1806 index SNPs, suggesting that MDD-specific genetic variants have an independent contribution to the aMCI-C (Table 2). Similarly, the PRS_{sAD} could significantly predict the aMCI-C ($P = 1.05 \times 10^{-9}$) and explained 18.09% of variance for the aMCI-C based on 49 504 index SNPs (Table 2). Additionally, PRS for MDD-specific and Alzheimer's disease-related genetic variants ($PRS_{sMDD+AD}$) could predict the aMCI-C ($P = 2.26 \times 10^{-10}$) and explained 19.17% of variance for the aMCI-C based on 50 527 index SNPs (Table 2). Compared to PRS_{AD} that explained 18.55% of variance for the aMCI-C, only 0.33% unique MDD variants were added to the $PRS_{sMDD+AD}$; however, the explained variance increased by 3.34%. To exclude the potential effects of known Alzheimer's disease genome regions, we removed SNPs located in 500 kb regions centred on the top 10 Alzheimer's disease loci (http://www.alzgene.org/) (Supplementary Table 3) and the predictive model of each PRS was still significant (Supplementary Table 4).

To validate the specificity of these index SNPs to MDD rather than Alzheimer's disease, LD score regression

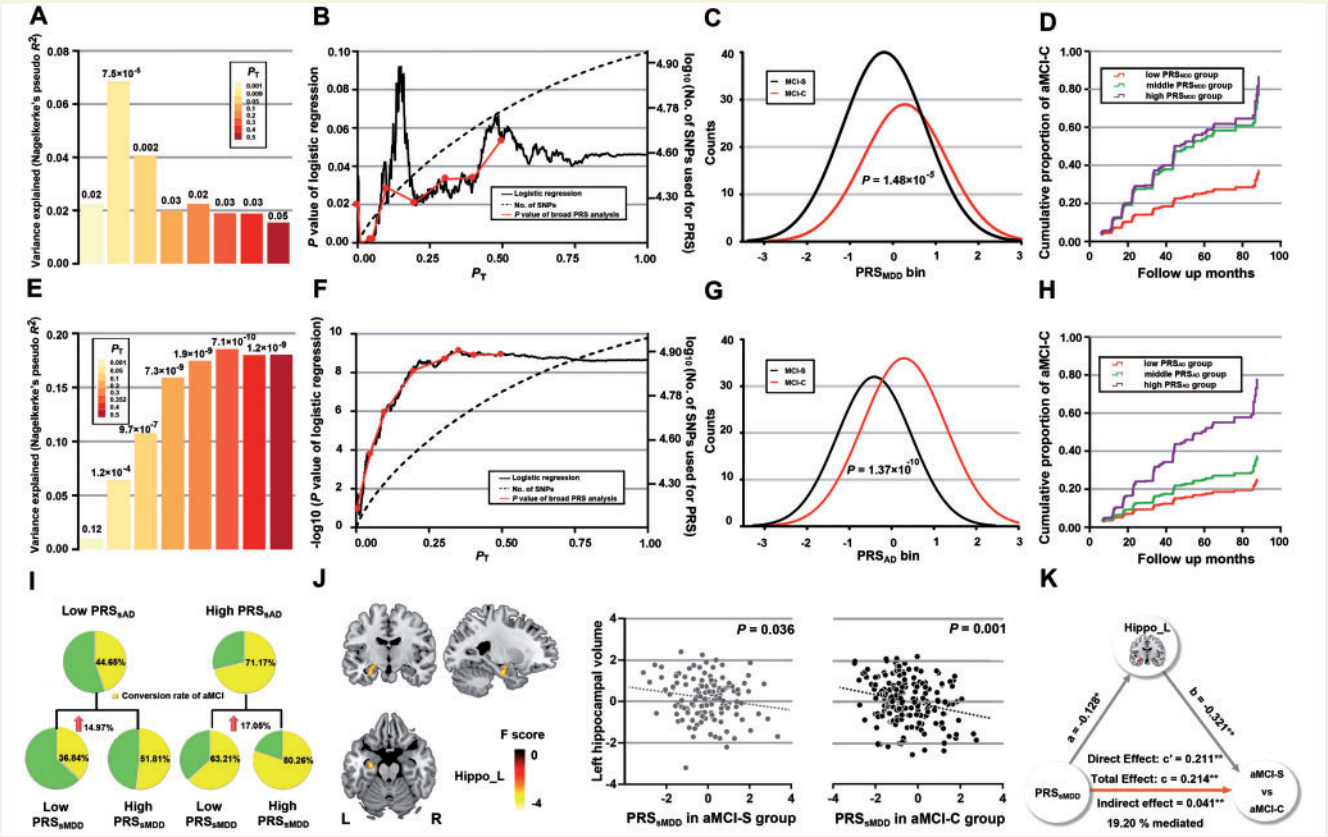

Figure 2 The predictive effects of PRS$_{MDD}$ (A–D) and PRS$_{AD}$ (E–H) on the conversion from aMCI to Alzheimer's disease, conversion rate among the bisected PRS groups (I) and mediation analysis (J–K). (**A** and **E**) The bar plots show the predictive effects of the PRS constructed by the best-fit P_T and other seven broad P_T values (0.001, 0.05, 0.1, 0.2, 0.3, 0.4 and 0.5) on the conversion of aMCI. The numbers above the bars are *P*-values for the logistic regression between the PRS and aMCI-C. The *y*-axis shows proportion of variance explained by the PRS. (**B** and **F**) The high resolution PRS analyses identify the best-fit P_T for constructing the PRS$_{MDD}$ (P_T = 0.009) and PRS$_{AD}$ (P_T = 0.352). The *x*-axis shows the P_T from 0.001 to 1 with an increment of 0.001. The black line shows the *P*-value of the logistic regression (left *y*-axis) at different P_T; the dashed line shows numbers of SNPs (right *y*-axis) at different P_T; and the red line connects points at the *P* values of the broad PRS analysis. (**C** and **G**) Distribution of the PRS measures for aMCI-S and aMCI-C. The *y*-axis shows the counts of each PRS bin (*x*-axis). (**D** and **H**) Cox proportional hazard model shows the associations between the PRS and the conversion from aMCI to Alzheimer's disease at different time points (*x*-axis). The *y*-axis shows the cumulative proportion of aMCI-C for any given follow-up period on the *x*-axis. The red, green and purple lines show the low, middle and high PRS groups, respectively. (**I**) Differences in conversion rate among the bisected PRS groups. (**J**) *Left*: The brain region with significant negative correlations between the PRS$_{sMDD}$ and GMV. *Right*: The scatter plots show correlations between the PRS$_{sMDD}$ and GMV in the aMCI-S and aMCI-C groups. (**K**) The mediation analysis shows that the left hippocampal volume mediates the predictive effect of the PRS$_{sMDD}$ on the conversion of aMCI. AD = Alzheimer's disease; P_T = *P*-values threshold of genome-wide association studies; *$P < 0.01$; **$P < 0.001$.

Table 2 The predictive effects of PRS on the conversion of aMCI (n = 322)

	P_T	SNPs	iSNPs	P	R^2, %	Specificity, %	Senstivitity, %	Accuracy, %	AUC
PRS$_{AD}$	0.352	2 622 845	49 831	7.10×10^{-10}	18.55	71.85	87.17	80.75	0.72
PRS$_{MDD}$	0.009	13 472	2559	7.49×10^{-5}	6.86	68.89	83.43	77.33	0.65
PRS$_{sAD}$	NA	2 618 134	49 504	1.05×10^{-9}	18.09	70.24	85.63	80.12	0.70
PRS$_{sMDD}$	NA	8761	1806	1.74×10^{-3}	4.19	65.11	81.74	76.01	0.62
PRS$_{sMDD+AD}$	NA	2 631 606	50 527	2.26×10^{-10}	19.17	70.37	88.24	81.06	0.75

AUC = area under curve of receiver operating characteristic curve; iSNPs = numbers of index single-nucleotide polymorphisms that constitute PRS; NA = not applicable; P_T = *P*-values threshold of genome-wide association studies; R^2 = Nagelkerke's pseudo R^2 of logistic regression; SNPs = numbers of single-nucleotide polymorphisms that constitute PRS.

showed that there was not any significant genetic correlation [$r_g = 0.69$, standard error (SE) = 1.32, $P = 0.60$] between MDD-specific genetic variants and Alzheimer's disease-related genetic variants. Using a Bayesian posterior probability of 0.90 as a cut-off threshold, there are 1582/1806 (87.5%) index SNPs that are highly associated with MDD (Supplementary Fig. 1A), but none of them are associated with Alzheimer's disease (Supplementary Fig. 1B), and none of these SNPs show significant colocalization between MDD and Alzheimer's disease (Supplementary Fig. 1C).

To balance the number of index SNPs used to construct the PRS, we created (i) PRS_{tsAD}, PRS_{AD} for the top 1806 Alzheimer's disease-specific index SNPs with the same numbers of index SNPs as the PRS_{sMDD}; and (ii) PRS_{sMDD} and PRS_{sAD} under the $P_T = 0.009$ (the same P_T as the PRS_{MDD}). We found that the predictive effect of PRS_{tsAD} and PRS_{sMDD} on conversion risk of aMCI were also significant (Supplementary material and Supplementary Table 5). These results indicate that the conversion from aMCI to Alzheimer's disease is related to only a small number of MDD-specific genetic variants but to a large number of Alzheimer's disease-specific genetic variants.

When the aMCI patients were divided into the low and high PRS_{sMDD} groups, the high PRS_{sMDD} group (65.38%) showed 16.25% higher conversion rate than the low PRS_{sMDD} group (49.13%) ($P = 0.002$). When patients were divided into the double low risk group, low PRS_{sAD} but high PRS_{sMDD} group, high PRS_{sAD} but low PRS_{sMDD} group, and double high risk group. There were significant differences in the conversion rate of the aMCI among these hierarchical PRS groups ($P = 4.26 \times 10^{-7}$). In the low PRS_{sAD} group, the aMCI patients with high PRS_{sMDD} showed marginally higher conversion rate than those with low PRS_{sMDD} (36.84% versus 51.81%, $P = 0.05$). In the high PRS_{sAD} group, the aMCI patients with high PRS_{sMDD} showed significantly higher conversion rate than those with low PRS_{sMDD} (63.21% versus 80.26%, $P = 0.002$) (Fig. 2I and Table 3). When PRS_{sMDD} and PRS_{sAD} were trisected into the low, middle and high risk, there were significant differences in conversion rate among the nine hierarchical PRS groups ($P = 3.23 \times 10^{-6}$) (Supplementary materials and Supplementary Table 6).

Table 3 Conversion rates of aMCI in the bisected PRS groups

PRS groups	aMCI-S, *n*	aMCI-C, *n*	Conversion rate, %
Low PRS_{sAD} and low PRS_{sMDD}	48	28	36.84
Low PRS_{sAD} and high PRS_{sMDD}	40	43	51.81
High PRS_{sAD} and low PRS_{sMDD}	32	55	63.21
High PRS_{sAD} and high PRS_{sMDD}	15	61	80.26
All	135	187	58.07

Hippocampal volume mediates association between PRS_{sMDD} and aMCI-C

To identify brain regions whose grey matter volumes were associated with PRS_{sMDD}, voxel-wise correlations were performed between PRS_{sMDD} and grey matter volume in the whole brain ($P_c < 0.05$, voxel-level FWE correction, cluster size > 200 voxels). The PRS_{sMDD} was negatively correlated with the grey matter volume of the left hippocampus (Brodmann area 36; peak MNI coordinate: $x = -27$, $y = -13.5$, $z = -21$; peak intensity = −5.329; 227 voxels; Fig. 2J).

Table 4 Top 10 neighbouring genes of the PPI network from PRS_{sMDD} fine-mapping of 1860 genes and PRS_{sMDD} fine-mapping of 1608 genes

Ranking	PRS_{sMDD} fine-mapping of 1860 genes[a]		PRS_{sMDD} fine-mapping of 1608 genes[b]	
	Gene symbol	Random walk probability	Gene symbol	Random walk probability
1	*APP*	6.84×10^{-3}	*APP*	6.78×10^{-3}
2	*ELAVL1*	4.49×10^{-3}	*ELAVL1*	4.49×10^{-3}
3	*NTRK1*	2.21×10^{-3}	*NXF1*	2.25×10^{-3}
4	*NXF1*	2.03×10^{-3}	*NTRK1*	2.17×10^{-3}
5	*CUL3*	1.70×10^{-3}	*CUL3*	1.71×10^{-3}
6	*MOV10*	1.50×10^{-3}	*MOV10*	1.50×10^{-3}
7	*TP53*	1.45×10^{-3}	*UBC*	1.46×10^{-3}
8	*EWSR1*	1.43×10^{-3}	*TR53*	1.32×10^{-3}
9	*UBC*	1.42×10^{-3}	*EWSR1*	1.19×10^{-3}
10	*TMEM17*	1.33×10^{-3}	*COPS5*	1.17×10^{-3}

[a]PRS_{sMDD} genetic variants were fine-mapped into 1860 genes based on the hippocampal-specific regulatory probability between eQTLs and epigenomic features (within a 5-kb window).
[b]PRS_{sMDD} genetic variants were fine-mapped into 1608 genes based on physical position of each variant (within a 5-kb window).
The abbreviation of genes is referred to at https://www.ncbi.nlm.nih.gov/gene/.

A total of 1806 index SNPs specific to MDD ($r^2 < 0.25$ within 250-kb window) were included in the calculation of PRS_{sMDD} after excluding genetic variants common to PRS_{MDD} ($P_T = 0.009$) and PRS_{AD} ($P_T = 0.352$). We set the PRS_{sMDD} as independent variable in the mediation analysis and instrumental variable in the Mendelian randomization analysis. In the mediation analysis, we found a significant direct effect from the PRS_{sMDD} to the aMCI group assignment ($P < 0.001$); from the PRS_{sMDD} to the left hippocampal volume ($P < 0.01$); and from the left hippocampal volume to the aMCI group assignment ($P < 0.001$). A significant indirect effect was also found in the left hippocampal volume ($P < 0.001$), which accounted for 19.20% of variance for the aMCI-C in this mediation model (Fig. 2K). In the conventional two-stage Mendelian randomization analysis, we found a negative association between PRS_{sMDD} and hippocampal volume ($\beta = -0.15$, SE = 0.06, $P = 0.01$); the predicted value of the left hippocampal volume was significantly associated with the aMCI-C ($\beta = -2.41$, OR = 0.09, SE = 0.78, $P = 0.002$). Mendelian randomization-Egger regression indicated no unbalanced horizontal pleiotropy (intercept = 0.011, $P = 0.07$) in the association between left hippocampal volume and aMCI conversion using PRS_{sMDD} as the instrumental variable. We also found significant causal effect of the left hippocampal volume on the aMCI conversion in the Mendelian randomization-Egger regression analysis ($\beta_{Egger} = -2.12$, OR = 0.12, SE = 0.77, $P = 0.002$). These results confirmed a causal chain from PRS_{sMDD} to hippocampal volume to conversion risk of aMCI.

Enrichment analyses using genes prioritized with hippocampal biological information

The 8762 SNPs used for calculating the PRS_{sMDD} were prioritized by integrating the hippocampus-specific eQTL and epigenomic features. The weight of the prioritization and the PGC-MDD GWAS *P*-value of each SNP were imported into the GATES software to fine-map these SNPs into 1860 significant genes (within a 5-kb window, 5705 SNPs located inside genes, $P < 0.001$).

To functionally annotate the 1860 genes, WebGestalt and GOrilla were applied to identify significant enrichment in GO and pathways (Fig. 3A–C and Supplementary Tables 7–9). In the annotation of GO, 505/1860 genes were enriched in the development process, 855/1860 in the protein binding, and 738/1860 in membrane part (Fig. 3A and Supplementary Table 7). Specifically, these genes mainly over-represented in biological processes of the anatomical structure morphogenesis ($q_c = 4.27 \times 10^{-5}$), cellular developmental process ($q_c = 7.08 \times 10^{-4}$) and development process ($q_c = 1.14 \times 10^{-3}$) (Fig. 3B and Supplementary Table 8), in the molecular function of the amyloid-β binding ($q_c = 8.64 \times 10^{-5}$), and in the cellular components of the neuron part ($q_c = 3.10 \times 10^{-11}$) and neuron projection ($q_c = 1.69 \times 10^{-5}$) (Fig. 3C and Supplementary Table 8). In the KEGG pathway analysis, these genes were enriched in neuronal development-related axon guidance ($q_c = 3.95 \times 10^{-3}$) (Fig. 3C and Supplementary Table 8). These functional annotations suggest that the PRS_{sMDD} genes were mainly related to the developmental process, and involved in the molecular binding between amyloid-β protein and its precursor, which is a well-known neuropathology of Alzheimer's disease.

To combine protein-level information, we mapped 1860 genes to the PPI network (642 unmatched genes were excluded). To illustrate potential functional connectivity of the remaindering 1218 genes, we used a network-based approach to identify a tightly connected PPI network (only 846 genes were included in the network). Using the network topology-based analysis, the top 10 neighbouring genes with the most functional similarity with seed genes were also included in the construction of the final PPI network consisting of 856 genes. As the most functionally neighbouring genes (Fig. 3D), the amyloid-β precursor protein (APP) formed the protein basis of the amyloid plaques in the brain of Alzheimer's disease patients. The 856 genes in the final PPI network were enriched mainly in development processes of the nervous system, such as nervous system development ($q_c = 2.83 \times 10^{-5}$), neuron projection development ($q_c = 9.08 \times 10^{-5}$), neuron projection guidance ($q_c = 4.20 \times 10^{-4}$), neurogenesis ($q_c = 6.51 \times 10^{-4}$) and generation of neurons ($q_c = 9.37 \times 10^{-4}$) (Fig. 3D and Supplementary Table 10).

The prior analyses indicate that PRS_{sMDD} fine-mapping genes are involved in brain developmental processes. We further explored in which developmental periods these genes were over-represented in the hippocampus. The CSEA online tool was used to explore the temporal-specific expression of these genes in the hippocampus. Under a pSI threshold of 0.05, 60 genes showed temporal-specific expression in the hippocampus in the middle-late foetal developmental period ($q_c = 6.02 \times 10^{-4}$) (Fig. 3E). Under the most stringent threshold (pSI = 0.001), only cell division cycle 20B (CDC20B) exhibited a temporal-specific high expression in the hippocampus in the middle-late foetal stage. The Human Brain Transcriptome dataset showed that the CDC20B was highly expressed in the early and late mid-foetal development period (Fig. 3E).

Among the nine major cell types in the mouse cortex and hippocampus, eight cell types exist in the hippocampal CA1 (Fig. 4A). The PRS_{sMDD} genes showed substantial over-representation mainly in the hippocampal pyramidal neurons ($q_c = 1.60 \times 10^{-7}$) and interneurons ($q_c = 3.61 \times 10^{-7}$) (Fig. 4B). However, these genes also demonstrated specific expression in the microglia cells ($q_c = 0.01$) and astrocytes ($q_c = 0.01$) (Fig. 4B).

Enrichment analyses using genes fine-mapped based on physical position

We also re-mapped 8762 MDD-specific SNPs into 1608 genes only based on the physical position of each

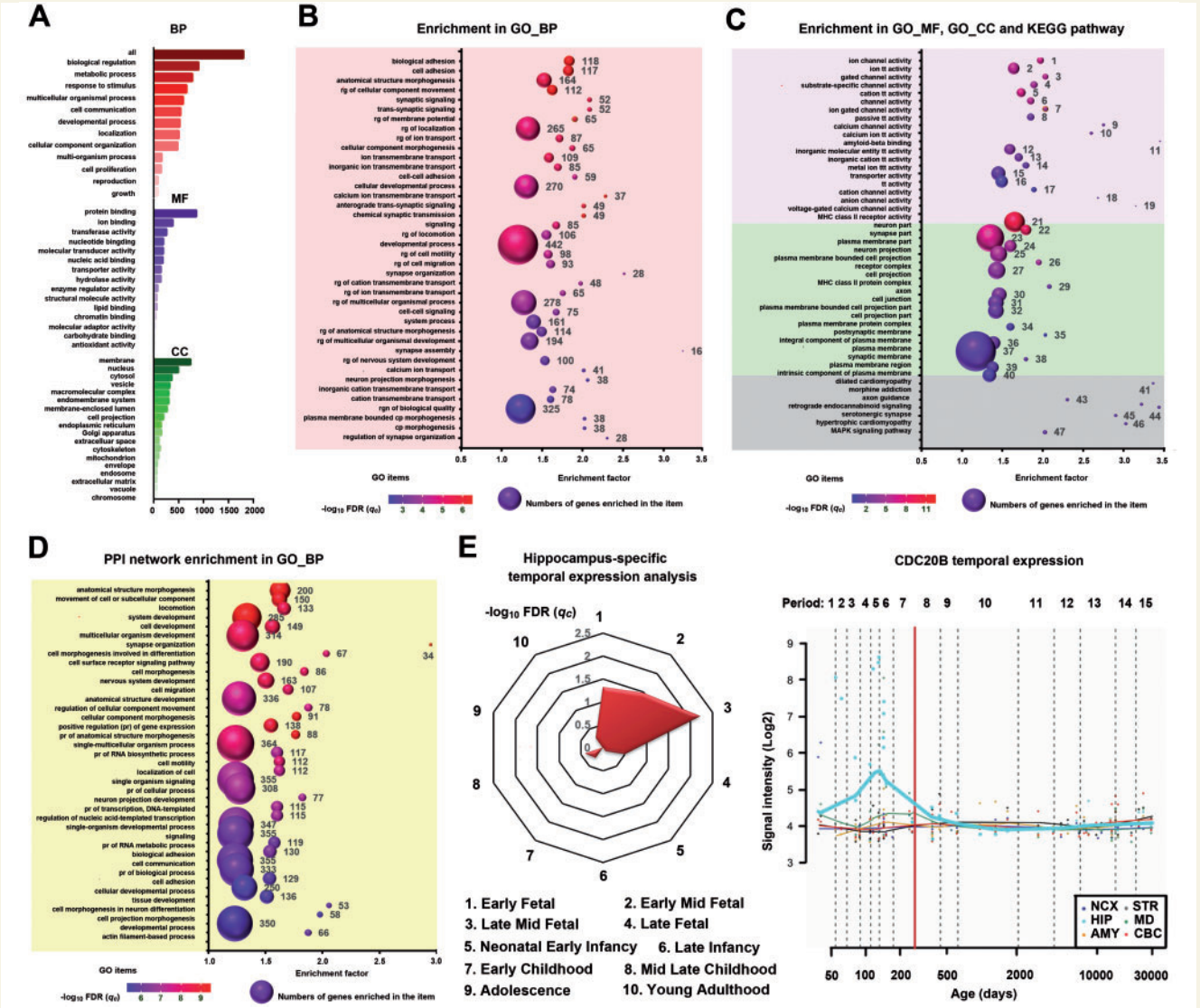

Figure 3 Gene enrichment of PRS_{sMDD} fine-mapping 1860 genes. (**A**) Enrichment of the PRS_{sMDD} genes in GO items. The *x*-axis shows the numbers of genes enriched in each item (*y*-axis). The red, purple, green bars denote the biological process, molecular function and cellular component, respectively. (**B**) Top 40 significant enriched GO biological process items of the PRS_{sMDD} genes. The *x*-axis shows enrichment factor of each GO item (*y*-axis). The size of the spheres reflects the number of genes (labelled beside the balls) enriched in each item. The colour of the spheres demonstrates the significance of the enrichment analyses. (**C**) Top 20 significant enriched GO molecular function and cellular component items, and all significant KEGG pathway items of the PRS_{sMDD} genes. The purple, green and grey background colours show the molecular function, cellular component and KEGG pathway, respectively. (**D**) Top 40 significant enriched GO biological process items of the PPI network. (**E**) *Left*: PRS_{sMDD} genes were highly expressed in the middle-late foetal developmental period in the hippocampus. *Right*: CDC20B was highly expressed in the early and late mid-foetal development periods in the hippocampus. Periods 1–15 are described in Supplementary Table 11. AMY = amygdala; BP = biological process; CBC = cerebellar cortex; CC = cellular component; CDC20B = cell division cycle 20B; cp = cell projection; GO = gene ontology; HIP = hippocampus; MF = molecular function; MD = mediodorsal nucleus of the thalamus; NCX = neocortex; pr = positive regulation; rg = regulation; STR = striatum; tt = transmembrane transporter.

variant (within 5-kb window). We found that 1468 genes were common between the two fine-mapping methods (with and without hippocampal biological information), suggesting that most genes related to these MDD-specific SNPs are associated with hippocampal gene expression. We performed enrichment analyses for the 1608 genes and found significant enrichment in developmental process and amyloid-β binding (Supplementary material, Supplementary Fig. 2 and Supplementary Tables 9 and 10).

Discussion

To our knowledge, this is the first study that integrates cross-scale neurobiological analyses and functional

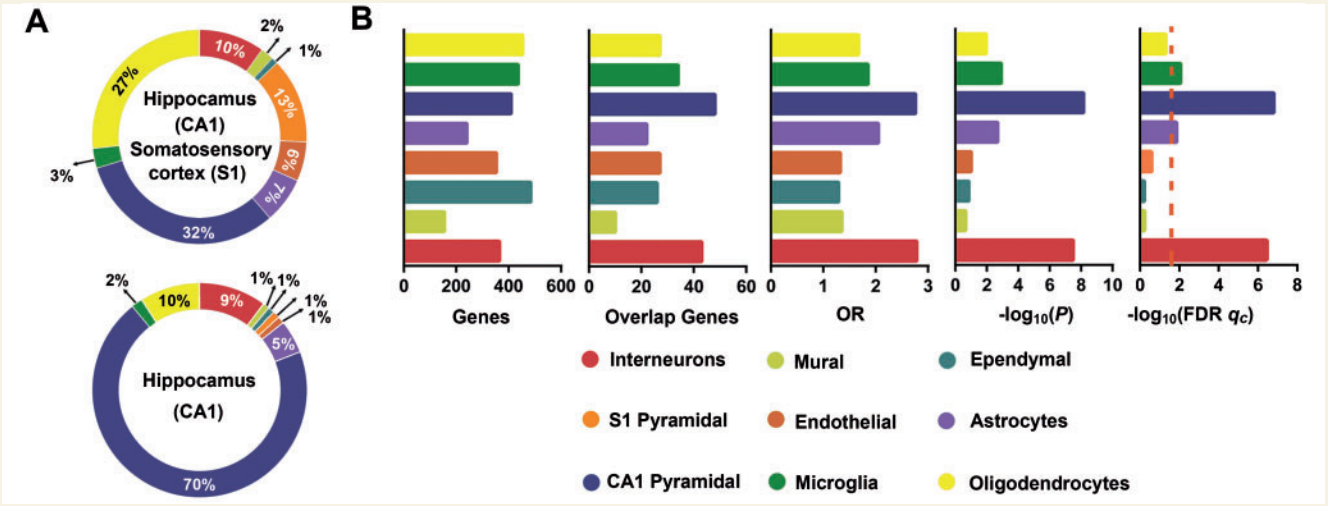

Figure 4 Cell type-specific expression analyses. (**A**) The frequency of the nine major cell types in the CA1 and S1 (*top*) and only in the CA1 (*bottom*) of the mouse brains (Zeisel *et al.*, 2015). (**B**) The first bar plot shows the numbers of genes in eight labelled cell types of hippocampus from the Zeisel *et al.* study. The second bar plot shows the numbers of overlapping genes between PRS$_{sMDD}$ fine-mapping 1860 genes and significantly expressed genes in each cell type of hippocampus. The last three bar plots show the cell type-specific expression results of the PRS$_{sMDD}$-related genes in the eight labelled cell types of the hippocampus. The dashed red line shows the significant level under $q_c < 0.05$ in FDR-BH correction. CA = cornu ammonis; GMV = grey matter volume; OR = odd ratios; S1 = somatosensory cortex.

annotations to investigate the independent predictive effect of MDD-specific genomic variants on the conversion from aMCI to Alzheimer's disease and the underlying neurobiological mechanisms. The PRS$_{sMDD}$ could predict the conversion by affecting the hippocampal volume. These genes were functionally related to the hippocampal development and amyloid-β binding. In addition, these genes showed temporal-specific expression in the hippocampus in the foetal developmental period and cell type-specific expression in the hippocampal pyramidal neurons and interneurons. These findings support a model of double attacks of hippocampus to explain for the neurobiological mechanisms of the independent contributions of MDD- and Alzheimer's disease-specific genomic variants to the conversion from aMCI to and Alzheimer's disease.

PRS$_{sMDD}$ could independently predict the conversion from aMCI to Alzheimer's disease

That Alzheimer's disease is a progressive polygenic disorder (Dubois *et al.*, 2007) and no effective therapies at the late stage makes early diagnosis and treatment to be the only way to improve prognosis (Chu, 2012). As the putative premorbid state of Alzheimer's disease (Mariani *et al.*, 2007), patients with aMCI have a high risk of developing into Alzheimer's disease (Palmer *et al.*, 2008). Because not all aMCI patients would convert to Alzheimer's disease, it is clinically important to predict the conversion from aMCI to Alzheimer's disease for early intervention. Consistent with previous studies (Rodriguez-Rodriguez *et al.*, 2013; Adams *et al.*, 2015), the PRS$_{AD}$ was found to predict conversion. More importantly, we found that the PRS$_{MDD}$ could also predict the conversion of non-depressed aMCI patients. Thus, the predictive ability of the PRS$_{MDD}$ cannot be explained by parallel depressive symptoms (Kida *et al.*, 2016; Mourao *et al.*, 2016; Sacuiu *et al.*, 2016; Barca *et al.*, 2017) and the coexistence of MDD (Modrego and Ferrandez, 2004). To exclude the possibility that the predictive effect of the PRS$_{MDD}$ is driven by genetic variants common to MDD and Alzheimer's disease, we found that the PRS$_{sMDD}$ could also predict the status of aMCI-C. LD score regression and co-localization analysis were performed to validate that these SNPs calculated for PRS$_{sMDD}$ are specific to MDD rather than Alzheimer's disease. Moreover, aMCI patients with high PRS$_{sMDD}$ showed 14.97% and 17.05% higher conversion rates than those with low PRS$_{sMDD}$ in the low and high PRS$_{sAD}$ groups, respectively. These findings suggest that the PRS$_{sMDD}$ has an independent contribution to the conversion from aMCI to Alzheimer's disease.

In terms of the clinical prediction for the conversion from aMCI to Alzheimer's disease, aMCI patients with the double high risk (high PRS$_{sMDD}$ and high PRS$_{sAD}$) showed a much higher conversion rate than those with the double low risk (low PRS$_{sMDD}$ and low PRS$_{sAD}$) (89.65% versus 33.33%). With the increased availability and decreasing cost of the sequencing technique, the genomic data of aMCI patients could be easily obtained, which could be used to construct the PRS$_{sMDD}$ and PRS$_{sAD}$ using the method of this study. In clinical practice, one could jointly use the PRS$_{sMDD}$ and PRS$_{sAD}$ to select aMCI patients with a much greater risk for Alzheimer's disease.

Appropriate intervention procedures for these aMCI patients may prevent or delay them from progressing into Alzheimer's disease.

Hippocampal volume mediates the prediction of PRS_{sMDD} in aMCI-C

Correlation, mediation and Mendelian randomization analyses revealed that hippocampal volume mediated the predictive effect of the PRS_{sMDD} on the conversion from aMCI to Alzheimer's disease. It has been recognized that reduced hippocampal volume is the most consistent subcortical abnormality in MDD patients in a meta-analysis of 1728 patients and 7199 controls (Schmaal *et al.*, 2016). The genetic variants have been proposed as an important cause for the reduced hippocampal volume in MDD. For example, MDD patients with risk alleles show a smaller hippocampal volume than those without risk alleles (Egan *et al.*, 2003; Frodl *et al.*, 2004, 2007, 2012; Kohli *et al.*, 2011). The reduction in hippocampal volume has been attributed to reduced gene expression in the hippocampus (Egan *et al.*, 2003; Kohli *et al.*, 2011). In children with few life stress events, the high PRS constructed by depression-related stress system genes could predict reduced hippocampal volume (Pagliaccio *et al.*, 2014). Moreover, in healthy individuals without depressive episodes, the depression-related risk-allele carriers also displayed a reduced hippocampal volume compared with non-carriers (Frodl *et al.*, 2008). These findings suggest that genetic variants for MDD could result in the reduction in the hippocampal volume in different populations.

It is well known that the volumetric reduction in the hippocampus is the most prominent early pathological feature of Alzheimer's disease (Yang *et al.*, 2012) and one of the most reliable predictive measures for the conversion from aMCI to Alzheimer's disease (Brueggen *et al.*, 2015). The additional burden to the hippocampus by MDD-specific genetic variants may exacerbate hippocampal atrophy and facilitate the conversion from aMCI to Alzheimer's disease. Thus, the model of double attacks on the hippocampus may explain the increased predictive value of the PRS_{sMDD} on the conversion from aMCI to Alzheimer's disease.

Neurobiological mechanisms underlying the predictive effect of PRS_{sMDD} on aMCI-C

To understand why hippocampal volume could mediate the predictive effect of the PRS_{sMDD} on conversion, the MDD-specific genetic variants were fine-mapped into the most common genes between the two different strategies (with and without hippocampal biological information), which suggested that most genes related to these MDD-specific SNPs are associated with hippocampal biological information.

The GO annotation revealed that MDD-related genes were related to amyloid-β binding, which is also supported by the PPI network analysis, showing that APP was the most important neighbouring gene in the network constructed by the MDD-related genes. The increased hippocampal amyloid-B, which is an important neuropathological change in Alzheimer's disease, is also related to depression (Rapp *et al.*, 2006) or depressive symptoms (Donovan *et al.*, 2018). These findings suggest that MDD-related genes may be involved in amyloid-β binding, an important neuropathological process of Alzheimer's disease.

The enrichment analysis of the biological process revealed that MDD-related genes were mainly involved in the nervous developmental process. The temporal-specific expression analysis further indicated that these genes were mainly expressed in the middle to late foetal periods in the hippocampus, which is in line with the critical developmental period of hippocampal neurons (Tran and Kelly, 2003). For example, CDC20B showed the highest expression in the hippocampus in the middle-late foetal periods (Fig. 3E). This gene is a developmental regulator of hippocampal neurons (Kim *et al.*, 2009; Yang *et al.*, 2010) and plays an essential role in dendritic morphogenesis (Kim *et al.*, 2009), axon growth (Yamada *et al.*, 2013) and presynaptic differentiation (Yang *et al.*, 2009), all of which are associated with hippocampal volume (Stockmeier *et al.*, 2004; Duman *et al.*, 2016). In addition, cell type-specific expression confirmed that these genes were mainly expressed in the hippocampal pyramidal neurons and interneurons. These findings suggest that MDD-related genes affect the hippocampal volume via modulating the gene expression of hippocampal neurons, which are the main cell types with prominent pathological impairment in Alzheimer's disease (Blazquez-Llorca *et al.*, 2011).

Limitations

Two limitations should be mentioned regarding this study. First, only volumetric measure was used as the intermediate phenotype. Consequently, we cannot exclude the possibility that other intermediate phenotypes may also mediate the association between PRS_{sMDD} and aMCI conversion. Second, the cell type-specific expression analysis was based on the hippocampus of mouse rather than human, because there are no publicly available cell type-specific expression data in the human hippocampus.

Conclusion

In this study, we found that the PRS_{sMDD} could independently predict conversion from aMCI to Alzheimer's disease, and the combined use of the PRS_{sMDD} and PRS_{sAD} could select aMCI patients with a much higher risk for conversion. The predictive effect of the PRS_{sMDD} on conversion

may be mediated by the hippocampus via affecting its early developmental process and amyloid-β binding.

Acknowledgements

We are grateful to the ADNI, IGAP and PGC consortium for providing summary statistics for the discovery and target sample. Data collection and sharing was funded by ADNI (National Institutes of Health U01 AG024904).

Funding

This work has been supported by the Natural Science Foundation of China (81425013, 81501451, 81501454, 81601476, 81701676, 81701668 and 81801687), Tianjin Key Technology R&D Program (17ZXMFSY00090), National Key Research and Development Program of China (2018YFC1314301), Postgraduate Innovation Fund of 13th Five-Year comprehensive investment of Tianjin Medical University (YJSCX201719), and Science&Technology Development Fund of Tianjin Education Commission for Higher Education (2016YD11).

Competing interests

The authors report no competing interests.

Supplementary material

Supplementary material is available at *Brain* online.

References

Adams HH, de Bruijn RF, Hofman A, Uitterlinden AG, van Duijn CM, Vernooij MW, et al. Genetic risk of neurodegenerative diseases is associated with mild cognitive impairment and conversion to dementia. Alzheimers Dement 2015; 11: 1277–85.

Barca ML, Persson K, Eldholm R, Benth JS, Kersten H, Knapskog AB, et al. Trajectories of depressive symptoms and their relationship to the progression of dementia. J Affect Disord 2017; 222: 146–52.

Blazquez-Llorca L, Garcia-Marin V, Merino-Serrais P, Avila J, DeFelipe J. Abnormal tau phosphorylation in the thorny excrescences of CA3 hippocampal neurons in patients with Alzheimer's disease. J Alzheimers Dis 2011; 26: 683–98.

Brown CD, Mangravite LM, Engelhardt BE. Integrative modeling of eQTLs and cis-regulatory elements suggests mechanisms underlying cell type specificity of eQTLs. PLoS Genet 2013; 9: e1003649.

Brueggen K, Dyrba M, Barkhof F, Hausner L, Filippi M, Nestor PJ, et al. Basal forebrain and hippocampus as predictors of conversion to alzheimer's disease in patients with mild cognitive impairment - a multicenter dti and volumetry study. J Alzheimers Dis 2015; 48: 197–204.

Bulik-Sullivan B, Finucane HK, Anttila V, Gusev A, Day FR, Loh PR, et al. An atlas of genetic correlations across human diseases and traits. Nat Genet 2015a; 47: 1236–41.

Bulik-Sullivan BK, Loh PR, Finucane HK, Ripke S, Yang J. LD Score regression distinguishes confounding from polygenicity in genome-wide association studies. Nat Genet 2015b; 47: 291–5.

Burgess S. Sample size and power calculations in Mendelian randomization with a single instrumental variable and a binary outcome. Int J Epidemiol 2014; 43: 922–9.

Burgess S, Thompson SG. Use of allele scores as instrumental variables for Mendelian randomization. Int J Epidemiol 2013; 42: 1134–44.

Burgess S, Thompson SG. Mendelian randomization: methods for using genetic variants in causal estimation. New York: Chapman and Hall/CRC; 2015.

Chu L. Alzheimer's disease: early diagnosis and treatment. Hong Kong Med J 2012; 18: 228–37.

De Roeck E, Ponjaert-Kristoffersen I, Bosmans M, De Deyn PP, Engelborghs S, Dierckx E. Are depressive symptoms in mild cognitive impairment predictive of conversion to dementia? Int Psychogeriatr 2016; 28: 921–8.

Donovan NJ, Locascio JJ, Marshall GA, Gatchel J, Hanseeuw BJ, Rentz DM, et al. Longitudinal association of amyloid beta and anxious-depressive symptoms in cognitively normal older adults. Am J Psychiatry 2018; 175: 530–7.

Dubois B, Feldman HH, Jacova C, DeKosky ST, Barberger-Gateau P, Cummings J, et al. Research criteria for the diagnosis of Alzheimer's disease: revising the NINCDS–ADRDA criteria. Lancet Neurol 2007; 6: 734–46.

Duman RS, Aghajanian GK, Sanacora G, Krystal JH. Synaptic plasticity and depression: new insights from stress and rapid-acting antidepressants. Nat Med 2016; 22: 238–49.

Eden E, Lipson D, Yogev S, Yakhini Z. Discovering motifs in ranked lists of DNA sequences. PLoS Comput Biol 2007; 3: e39.

Eden E, Navon R, Steinfeld I, Lipson D, Yakhini Z. GOrilla: a tool for discovery and visualization of enriched GO terms in ranked gene lists. BMC Bioinformatics 2009; 10: 48.

Egan MF, Kojima M, Callicott JH, Goldberg TE, Kolachana BS, Bertolino A, et al. The BDNF val66met polymorphism affects activity-dependent secretion of BDNF and human memory and hippocampal function. Cell 2003; 112: 257–69.

Escott-Price V, Sims R, Bannister C, Harold D, Vronskaya M, Majounie E, et al. Common polygenic variation enhances risk prediction for Alzheimer's disease. Brain 2015; 138: 3673–84.

Euesden J, Lewis CM, O'Reilly PF. PRSice: polygenic risk score software. Bioinformatics 2015; 31: 1466–8.

Frodl T, Carballedo A, Hughes MM, Saleh K, Fagan A, Skokauskas N, et al. Reduced expression of glucocorticoid-inducible genes GILZ and SGK-1: high IL-6 levels are associated with reduced hippocampal volumes in major depressive disorder. Trans Psychiatry 2012; 2: e88.

Frodl T, Koutsouleris N, Bottlender R, Born C, Jager M, Morgenthaler M, et al. Reduced gray matter brain volumes are associated with variants of the serotonin transporter gene in major depression. Mol Psychiatry 2008; 13: 1093–101.

Frodl T, Meisenzahl EM, Zill P, Baghai T, Rujescu D, Leinsinger G, et al. Reduced hippocampal volumes associated with the long variant of the serotonin transporter polymorphism in major depression. Arch Gen Psychiatry 2004; 61: 177–83.

Frodl T, Schule C, Schmitt G, Born C, Baghai T, Zill P, et al. Association of the brain-derived neurotrophic factor Val66Met polymorphism with reduced hippocampal volumes in major depression. Arch Gen Psychiatry 2007; 64: 410–16.

Giambartolomei C, Vukcevic D, Schadt EE, Franke L, Hingorani AD, Wallace C, et al. Bayesian test for colocalisation between pairs of genetic association studies using summary statistics. PLoS Genet 2014; 10: e1004383.

Gibson J, Russ TC, Adams MJ, Clarke TK, Howard DM, Hall LS, et al. Assessing the presence of shared genetic architecture between Alzheimer's disease and major depressive disorder using genome-wide association data. Transl Psychiatry 2017; 7: e1094.

Hames JL, Hagan CR, Joiner TE. Interpersonal processes in depression. Annu Rev Clin Psychol 2013; 9: 355–77.
Hayes AF. Introduction to mediation, moderation, and conditional process analysis: a regression-based approach. New York: Guilford Press; 2013.
Holmes AJ, Lee PH, Hollinshead MO, Bakst L, Roffman JL, Smoller JW, et al. Individual differences in amygdala-medial prefrontal anatomy link negative affect, impaired social functioning, and polygenic depression risk. J Neurosci 2012; 32: 18087–100.
Howie B, Fuchsberger C, Stephens M, Marchini J, Abecasis GR. Fast and accurate genotype imputation in genome-wide association studies through pre-phasing. Nat Genet 2012; 44: 955–9.
Jack CR Jr, Bernstein MA, Fox NC, Thompson P, Alexander G, Harvey D, et al. The Alzheimer's Disease Neuroimaging Initiative (ADNI): MRI methods. J Magn Reson Imaging 2008; 27: 685–91.
Jorm AF. History of depression as a risk factor for dementia: an updated review. Aust N Z J Psychiatry 2001; 35: 776–81.
Julayanont P, Brousseau M, Chertkow H, Phillips N, Nasreddine ZS. Montreal Cognitive Assessment Memory Index Score (MoCA-MIS) as a predictor of conversion from mild cognitive impairment to Alzheimer's disease. J Am Geriatr Soc 2014; 62: 679–84.
Kang HJ, Kawasawa YI, Cheng F, Zhu Y, Xu X, Li M, et al. Spatio-temporal transcriptome of the human brain. Nature 2011; 478: 483–9.
Kida J, Nemoto K, Ikejima C, Bun S, Kakuma T, Mizukami K, et al. Impact of depressive symptoms on conversion from mild cognitive impairment subtypes to alzheimer's disease: a community-based longitudinal study. J Alzheimers Dis 2016; 51: 405–415.
Kim AH, Puram SV, Bilimoria PM, Ikeuchi Y, Keough S, Wong M, et al. A centrosomal Cdc20-APC pathway controls dendrite morphogenesis in postmitotic neurons. Cell 2009; 136: 322–36.
Kohler S, Bauer S, Horn D, Robinson PN. Walking the interactome for prioritization of candidate disease genes. Am J Hum Genet 2008; 82: 949–58.
Kohli MA, Lucae S, Saemann PG, Schmidt MV, Demirkan A, Hek K, et al. The neuronal transporter gene SLC6A15 confers risk to major depression. Neuron 2011; 70: 252–65.
Kundaje A, Meuleman W, Ernst J, Bilenky M, Yen A, Heravi-Moussavi A, et al. Integrative analysis of 111 reference human epigenomes. Nature 2015; 518: 317–30.
Lambert JC, Ibrahim-Verbaas CA, Harold D, Naj AC, Sims R, Bellenguez C, et al. Meta-analysis of 74,046 individuals identifies 11 new susceptibility loci for Alzheimer's disease. Nat Genet 2013; 45: 1452–8.
Li MJ, Li M, Liu Z, Yan B, Pan Z, Huang D, et al. cepip: context-dependent epigenomic weighting for prioritization of regulatory variants and disease-associated genes. Genome Biol 2017; 18: 52.
Li MX, Gui HS, Kwan JS, Sham PC. GATES: a rapid and powerful gene-based association test using extended Simes procedure. Am J Hum Genet 2011; 88: 283–93.
Li Y, Willer CJ, Ding J, Scheet P, Abecasis GR. MaCH: using sequence and genotype data to estimate haplotypes and unobserved genotypes. Genet Epidemiol 2010; 34: 816–34.
Mariani E, Monastero R, Mecocci P. Mild cognitive impairment: a systematic review. J Alzheimers Dis 2007; 12: 23–35.
Mazzeo S, Santangelo R, Bernasconi MP, Cecchetti G, Fiorino A, Pinto P, et al. Combining cerebrospinal fluid biomarkers and neuropsychological assessment: a simple and cost-effective algorithm to predict the progression from mild cognitive impairment to alzheimer's disease dementia. J Alzheimers Dis 2016; 54: 1495–508.
Milaneschi Y, Lamers F, Peyrot WJ, Abdellaoui A, Willemsen G, Hottenga JJ, et al. Polygenic dissection of major depression clinical heterogeneity. Mol Psychiatry 2016; 21: 516–22.
Modrego PJ, Ferrandez J. Depression in patients with mild cognitive impairment increases the risk of developing dementia of Alzheimer type: a prospective cohort study. Arch Neurol 2004; 61: 1290–3.
Mormino EC, Sperling RA, Holmes AJ, Buckner RL, De Jager PL, Smoller JW, et al. Polygenic risk of Alzheimer disease is associated with early- and late-life processes. Neurology 2016; 87: 481–8.
Mourao RJ, Mansur G, Malloy-Diniz LF, Castro Costa E, Diniz BS. Depressive symptoms increase the risk of progression to dementia in subjects with mild cognitive impairment: systematic review and meta-analysis. Int J Geriatr Psychiatry 2016; 31: 905–11.
Pagliaccio D, Luby JL, Bogdan R, Agrawal A, Gaffrey MS, Belden AC, et al. Stress-system genes and life stress predict cortisol levels and amygdala and hippocampal volumes in children. Neuropsychopharmacology 2014; 39: 1245.
Palmer K, Backman L, Winblad B, Fratiglioni L. Mild cognitive impairment in the general population: occurrence and progression to Alzheimer disease. Am J Geriatr Psychiatry 2008; 16: 603–11.
Palmer K, Di Iulio F, Varsi AE, Gianni W, Sancesario G, Caltagirone C, et al. Neuropsychiatric predictors of progression from amnestic-mild cognitive impairment to Alzheimer's disease: the role of depression and apathy. J Alzheimers Dis 2010; 20: 175–83.
Park S, Hatim A, Si TM, Jeon HJ, Srisurapanont M, Bautista D, et al. Stressful life events preceding the onset of depression in Asian patients with major depressive disorder. Int J Soc Psychiatry 2015; 61: 735–42.
Pickrell JK, Berisa T, Liu JZ. Detection and interpretation of shared genetic influences on 42 human traits. Nat Genet 2016; 48: 709–17.
Power RA, Tansey KE, Buttenschon HN, Cohen-Woods S, Bigdeli T, Hall LS, et al. Genome-wide association for major depression through age at onset stratification: major depressive disorder working group of the psychiatric genomics consortium. Bio Psychiatry 2017; 81: 325–35.
Preacher KJ, Hayes AF. Asymptotic and resampling strategies for assessing and comparing indirect effects in multiple mediator models. Behav Res Methods 2008; 40: 879–91.
Purcell SM, Wray NR, Stone JL, Visscher PM, O'Donovan MC, Sullivan PF, et al. Common polygenic variation contributes to risk of schizophrenia and bipolar disorder. Nature 2009; 460: 748–52.
Qiu A, Shen M, Buss C, Chong YS, Kwek K, Saw SM, et al. Effects of antenatal maternal depressive symptoms and socio-economic status on neonatal brain development are modulated by genetic risk. Cereb Cortex 2017; 27: 3080–92.
Rapp MA, Schnaider-Beeri M, Grossman HT, Sano M, Perl DP, Purohit DP, et al. Increased hippocampal plaques and tangles in patients with Alzheimer disease with a lifetime history of major depression. Arch Gen Psychiatry 2006; 63: 161–7.
Ripke S, Wray NR, Lewis CM, Hamilton SP, Weissman MM, Breen G, et al. A mega-analysis of genome-wide association studies for major depressive disorder. Mol Psychiatry 2013; 18: 497–511.
Rodriguez-Rodriguez E, Sanchez-Juan P, Vazquez-Higuera JL, Mateo I, Pozueta A, Berciano J, et al. Genetic risk score predicting accelerated progression from mild cognitive impairment to Alzheimer's disease. J Neural Transm 2013; 120: 807–12.
Sabuncu MR, Buckner RL, Smoller JW, Lee PH, Fischl B, Sperling RA. The association between a polygenic Alzheimer score and cortical thickness in clinically normal subjects. Cereb Cortex 2012; 22: 2653–61.
Sacuiu S, Insel PS, Mueller S, Tosun D, Mattsson N, Jack CR Jr, et al. chronic depressive symptomatology in mild cognitive impairment is associated with frontal atrophy rate which hastens conversion to alzheimer dementia. Am J Geriatr Psychiatry 2016; 24: 126–35.
Schmaal L, Veltman DJ, van Erp TG, Samann PG, Frodl T, Jahanshad N, et al. Subcortical brain alterations in major depressive disorder: findings from the ENIGMA major depressive disorder working group. Mol Psychiatry 2016; 21: 806–12.
Skoog I, Waern M, Duberstein P, Blennow K, Zetterberg H, Borjesson-Hanson A, et al. A 9-year prospective population-based study on the association between the APOE*E4 allele and late-life depression in Sweden. Bio Psychiatry 2015; 78: 730–6.

Stockmeier CA, Mahajan GJ, Konick LC, Overholser JC, Jurjus GJ, Meltzer HY, et al. Cellular changes in the postmortem hippocampus in major depression. Bio Psychiatry 2004; 56: 640–50.

Sullivan PF. The psychiatric GWAS consortium: big science comes to psychiatry. Neuron 2010; 68: 182–6.

Tokuchi R, Hishikawa N, Kurata T, Sato K, Kono S, Yamashita T, et al. Clinical and demographic predictors of mild cognitive impairment for converting to Alzheimer's disease and reverting to normal cognition. J Neurol Sci 2014; 346: 288–92.

Tran TD, Kelly SJ. Critical periods for ethanol-induced cell loss in the hippocampal formation. Neurotoxicol Teratol 2003; 25: 519–28.

Wang J, Vasaikar S, Shi Z, Greer M, Zhang B. WebGestalt 2017: a more comprehensive, powerful, flexible and interactive gene set enrichment analysis toolkit. Nucleic Acids Res 2017; 45: W130–7.

Winblad B, Palmer K, Kivipelto M, Jelic V, Fratiglioni L, Wahlund LO, et al. Mild cognitive impairment–beyond controversies, towards a consensus: report of the international working group on mild cognitive impairment. J Intern Med 2004; 256: 240–6.

Wyman BT, Harvey DJ, Crawford K, Bernstein MA, Carmichael O, Cole PE, et al. Standardization of analysis sets for reporting results from ADNI MRI data. Alzheimers Dement 2013; 9: 332–7.

Xu X, Wells AB, O'Brien DR, Nehorai A, Dougherty JD. Cell type-specific expression analysis to identify putative cellular mechanisms for neurogenetic disorders. J Neurosci 2014; 34: 1420–31.

Yamada T, Yang Y, Bonni A. Spatial organization of ubiquitin ligase pathways orchestrates neuronal connectivity. Trends Neurosci 2013; 36: 218–26.

Yang J, Pan P, Song W, Huang R, Li J, Chen K, et al. Voxelwise meta-analysis of gray matter anomalies in Alzheimer's disease and mild cognitive impairment using anatomic likelihood estimation. J Neurol Sci 2012; 316: 21–9.

Yang Y, Kim AH, Bonni A. The dynamic ubiquitin ligase duo: Cdh1-APC and Cdc20-APC regulate neuronal morphogenesis and connectivity. Curr Opin Neurobiol 2010; 20: 92–9.

Yang Y, Kim AH, Yamada T, Wu B, Bilimoria PM, Ikeuchi Y, et al. A Cdc20-APC ubiquitin signaling pathway regulates presynaptic differentiation. Science 2009; 326: 575–8.

Ye Q, Bai F, Zhang Z. shared genetic risk factors for late-life depression and Alzheimer's disease. J Alzheimers Dis 2016; 52: 1–15.

Yuan Y, Gu ZX, Wei WS. Fluorodeoxyglucose-positron-emission tomography, single-photon emission tomography, and structural MR imaging for prediction of rapid conversion to Alzheimer disease in patients with mild cognitive impairment: a meta-analysis. AJNR Am J Neuroradiol 2009; 30: 404–10.

Zeisel A, Munoz-Manchado AB, Codeluppi S, Lonnerberg P, La Manno G, Jureus A, et al. Brain structure. Cell types in the mouse cortex and hippocampus revealed by single-cell RNA-seq. Science 2015; 347: 1138–42.